Solid-State Structures

DOI: 10.1002/ange.201310110

Ruthenium(V) Oxides from Low-Temperature Hydrothermal Synthesis**

*Craig I. Hiley, Martin R. Lees, Janet M. Fisher, David Thompsett, Stefano Agrestini, Ronald I. Smith, and Richard I. Walton**

Abstract: *Low-temperature (200°C) hydrothermal synthesis of the ruthenium oxides $Ca_{1.5}Ru_2O_7$, $SrRu_2O_6$, and $Ba_2Ru_3O_9(OH)$ is reported. $Ca_{1.5}Ru_2O_7$ is a defective pyrochlore containing $Ru^{V/VI}$; $SrRu_2O_6$ is a layered Ru^V oxide with a $PbSb_2O_6$ structure, whilst $Ba_2Ru_3O_9(OH)$ has a previously unreported structure type with orthorhombic symmetry solved from synchrotron X-ray and neutron powder diffraction. $SrRu_2O_6$ exhibits unusually high-temperature magnetic order, with antiferromagnetism persisting to at least 500 K, and refinement using room temperature neutron powder diffraction data provides the magnetic structure. All three ruthenates are metastable and readily collapse to mixtures of other oxides upon heating in air at temperatures around 300–500°C, suggesting they would be difficult, if not impossible, to isolate under conventional high-temperature solid-state synthesis conditions.*

Oxides of ruthenium find use in topical areas of electrocatalysis for water oxidation and reduction,[1–3] in heterogeneous catalysis,[1,4] and the magnetic properties of 4d and 5d metal oxides are more generally the focus of much current attention because of their distinct phenomena arising from strong spin–orbit coupling not seen in 3d metal oxides.[5] The majority of oxides of ruthenium contain Ru^{IV}, and isolation of the relatively unstable oxidation states +5 or higher typically requires highly oxidizing synthesis conditions, such as oxygen pressure.[6–9] As with many multi-element oxides, synthesis is dominated by the use of high temperature (>1200°C), and this means that usually only the most thermodynamically stable compounds are isolated.[10] Thus potentially large numbers of metastable oxide phases remain undiscovered, particularly for the 4d and 5d transition elements whose chemistry is less explored than the first-row elements, and for which the use of mild reaction conditions may allow access to.[11,12] A range of complex ruthenium oxides containing Ca, Sr, or Ba have been reported and are of interest for their diverse and unusual magnetic and electronic properties. For example, Sr_2RuO_4 is a notable example of a Cu-free high temperature superconductor,[13] whilst $SrRuO_3$ is both a metallic conductor and ferromagnetic.[14,15] Munenaka and Sato previously reported the high temperature (600°C) hydrothermal synthesis of the Ru^V pyrochlore $Ca_2Ru_2O_7$,[16] which exhibits magnetic properties of a spin-glass.[17] Compared to traditional, solid-state techniques, hydrothermal synthesis generally utilizes much lower temperatures, to allow metastable compounds, potentially containing unusual oxidation states of metals, to be prepared.[18] In previous work we considered the formation of iridium oxides by direct crystallization from aqueous solution at temperatures less than 250°C.[19,20] Herein we report details of the synthesis and characterization of three previously unreported Ru^V containing oxides. They are prepared under highly oxidizing aqueous conditions by the hydrothermal reaction of $KRu^{VII}O_4$ and an alkaline earth metal peroxide, MO_2 (M = Ca, Sr, Ba) at 200°C (see the Experimental Section). The novelty of our approach lies in its simplicity: only two inorganic precursors are used, in stoichoimetric proportions, with no additional mineralizers or pH modifiers (unlike many other hydrothermal crystallizations), and this allows reproducible formation of highly crystalline phases. Furthermore the temperatures used are significantly lower than those used in other "soft chemical" synthesis of ruthenates; in molten hydroxide or carbonate fluxes, for example, temperatures above 600°C are reported to bring about crystallization.[21,22]

[*] C. I. Hiley, Prof. R. I. Walton
Department of Chemistry, University of Warwick
Gibbet Hill Road, Coventry, CV4 7AL (UK)
E-mail: r.i.walton@warwick.ac.uk
Dr. M. R. Lees
Department of Physics, University of Warwick
Gibbet Hill Road, Coventry, CV4 7AL (UK)
Dr. J. M. Fisher, Dr. D. Thompsett
Johnson Matthey Technology Centre
Sonning Common, Reading, RG4 9NH (UK)
Dr. S. Agrestini
Max-Planck Institut, CPfS
Nöthnitzer Strasse 40, 01187 Dresden (Germany)
Dr. R. I. Smith
ISIS Neutron and Muon Source, Rutherford Appleton Laboratory
Harwell Oxford, Didcot, OX11, 0QX (UK)

[**] We thank Johnson Matthey Plc for the provision of a CASE studentship for C.I.H. Some of the equipment used in materials characterization at the University of Warwick was obtained through the Science City Advanced Materials project "Creating and Characterising Next Generation Advanced Materials" with support from Advantage West Midlands (AWM) and part funded by the European Regional Development Fund (ERDF). We are grateful to Diamond Light Source for provision of beamtime for the XANES and synchrotron XRD experiments, and to the STFC for neutron diffraction experiments at ISIS, including the GEM Xpress service. We thank Dr. H. Y. Playford, Dr. A. J. Dent, L. M. Daniels, Dr. C. C. Tang, Dr. A. S. Munn, and M. I. Breeze for help with data collection at these facilities. Thanks are also expressed to D. L. Burnett for help with microscopy, L. M. Daniels for TGA, and to I. Briggs and A. M. Rusu for ICP elemental analysis.

Supporting information for this article is available on the WWW under http://dx.doi.org/10.1002/anie.201310110.

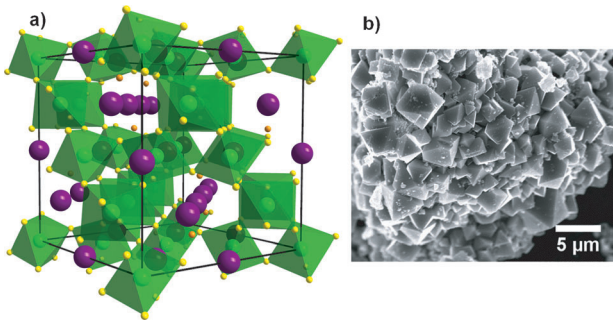

Figure 1. a) The $A_2B_2O_6O'$pyrochlore unit cell of $Ca_{1.5}Ru_2O_7$, with green RuO_6 octahedra, orange O′ sites, and partially occupied Ca sites shown in purple. b) A scanning electron micrograph of octahedral crystals of the material.

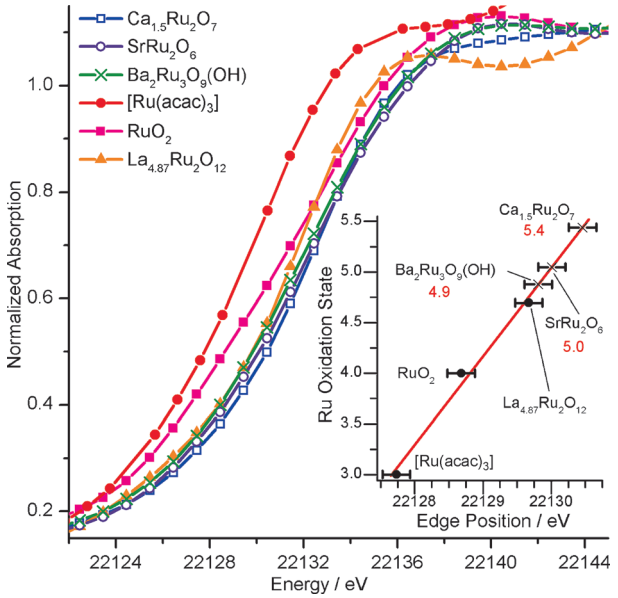

Figure 2. Normalized Ru K-edge XANES spectra of $Ca_{1.5}Ru_2O_7$, $SrRu_2O_6$, $Ba_2Ru_2O_9(OH)$, and reference compounds of known oxidation state ($[Ru^{III}(acac)_3]$, $Ru^{IV}O_2$, $La_{4.87}Ru^{4.7}{}_2O_{12}$). Inset: a plot of edge position (defined as the energy at which absorption = 0.5) as a function of oxidation state with linear fit of reference compounds, which is used to estimate the Ru oxidation state (in red) in the Sr, Ca, and Ba ruthenates.

The hydrothermal reaction between CaO_2 and $KRuO_4$ forms a pyrochlore,[23] space group $Fd\bar{3}m$, $a = 10.1997(1)$ Å (Figure 1), with a composition of $Ca_{1.5}Ru_2O_7$ derived from Rietveld refinements using neutron time-of-flight powder diffraction data (Supporting Information, Figure S2). Elemental analysis using ICP-OES confirms a Ca to Ru ratio of 0.75:1. Such a defective pyrochlore structure is not without precedent: for example several $A(BB')O_6$ pyrochlores with half occupied A-site and a mixed-metal B-site have been reported.[24] The absence of A-site water or hydroxide for the calcium ruthenate was confirmed by IR spectroscopy and thermogravimetric analysis (TGA; Supporting Information, Figures S1 and S7). Furthermore, there is no indication of any oxide vacancies in the structure from the refinement using powder neutron diffraction, and therefore to achieve charge balance we assign a mixed (V,VI) oxidation state of Ru. Ru K-edge X-ray absorption near-edge spectroscopy, XANES, (Figure 2) confirms an average oxidation state of close to 5.5. Bond valence calculations[25] using a bond valence parameter for Ru^V derived by Dussarrat et al.[10] yield a Ru oxidation state of 5.19. Addition of excess CaO_2 to the hydrothermal synthesis does not alter the composition of the pyrochlore and instead forms $Ca(OH)_2$ as a by-product. Upon heating in air, in situ powder X-ray diffraction (XRD) and TGA reveals that at temperatures as low as 300 °C, phase separation begins to occur with the appearance of RuO_2 leading to a mixture of RuO_2 and the stoichiometric pyrochlore $Ca_2Ru_2O_7$ (Supporting Information, Figure S5). Further heating in air to 750 °C triggers the collapse and phase separation of the pyrochlore to the perovskite $CaRuO_3$ and rutile RuO_2 with complete reduction of the ruthenium(V) to ruthenium(IV).

The hydrothermal reaction of SrO_2 and two equivalents of $KRuO_4$ yields phase-pure, hexagonal plates of $SrRu_2O_6$ (Figure 3c). $SrRu_2O_6$ adopts the hexagonal lead antimonate structure ($PbSb_2O_6$, $P\bar{3}1m$, $a = 5.20573(3)$, $c = 5.23454(7)$ Å), consisting of alternating layers of edge-sharing RuO_6 octahedra and interlayed Sr^{2+} ions that are also octahedrally coordinated (Figure 3a,b). $SrRu_2O_6$ is a rare example of a $PbSb_2O_6$ structure type that contains a magnetic transition-metal ion, the only other known examples being UM_2O_6 (M = Cr,V)[26] and $PdAs_2O_6$.[27] Ru K-edge XANES proves the average oxidation state of 5 (Figure 2), which is also confirmed by its bond valence sum (5.17). Room-temperature neutron diffraction data (Figure 4) reveals several Bragg peaks not seen in the powder XRD pattern, which can be explained by magnetic scattering of an antiferromagnetic array of Ru^V centers. The magnetic scattering can be indexed to a hexagonal unit cell with lattice parameters $a = 5.20573(3)$, $c = 10.46908(14)$ Å in the space group, $P\bar{3}1c$ (that is, doubled along c) with the Ru atoms antiferromagnetically coupled both in the ab plane (intralayer) and parallel to the c-axis (interlayer; Figure 4, inset). The magnetic moment is along the c direction and has a refined magnitude of 2.39 μ_B. This value is very close to the value previously reported for Ru^{5+}, 2.43–2.54 μ_B, in a doped double perovskite[28] and is comparable to the moment reported for the isoelectronic, octahedral Tc^{4+} in the perovskite $SrTcO_3$ (1.87 μ_B at room temperature).[29] These moments are both smaller than the spin-only value, which may be due to a large degree of covalency in M–O bonds for 4d metals.[30] Both $SrRu_2O_6$ and $SrTcO_3$ exhibit magnetic order above room temperature and for $SrTcO_3$ electronic structure calculations revealed this is due to the proximity of the half-filled t_{2g} shells to an itinerant-to-localized transition.[31] In situ powder XRD upon heating in air shows that at around 400 °C $SrRu_2O_6$ decomposes to $SrRuO_3$ and RuO_2 (Supporting Information, Figure S8).

A 2:3 molar ratio of BaO_2 and $KRuO_4$ reacts under hydrothermal conditions at 200 °C to give a phase-pure sample of the new phase $Ba_2Ru_3O_9(OH)$ as plate-like crystallites. This was indexed to the orthorhombic space group $P2_12_12_1$, $a = 12.19451(1)$, $b = 9.87825(1)$, and $c = 7.05847(1)$ Å (Figure 5a) from synchrotron radiation powder XRD. Figure 6 shows the refined crystal structure,

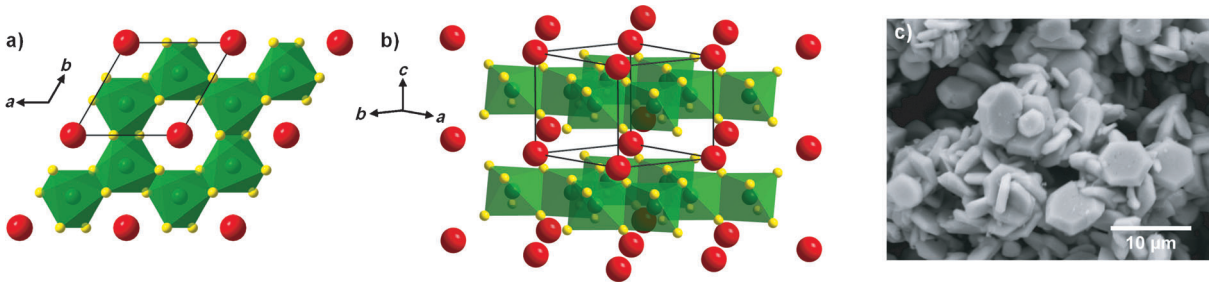

Figure 3. a) The structure of $SrRu_2O_6$, as viewed in the *ab* plane; b) a representation showing the layered structure with green RuO_6 octahedra and red Sr^{2+} ions; c) a scanning electron micrograph of $SrRu_2O_6$ crystals.

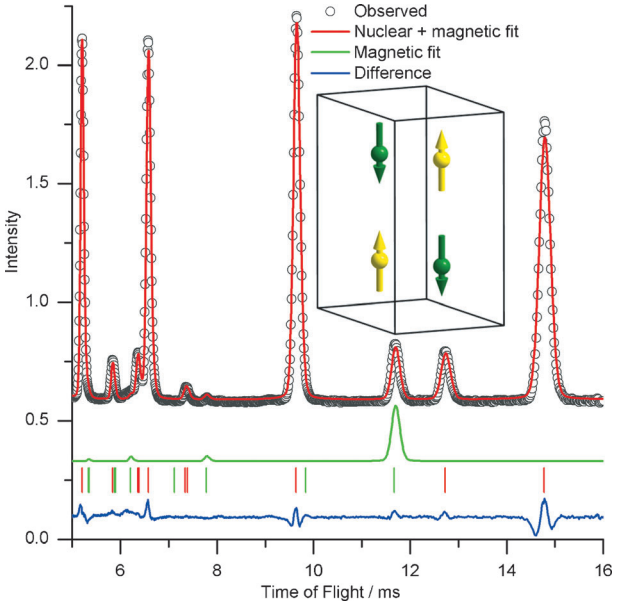

Figure 4. Rietveld refinement of the nuclear and magnetic structure from room temperature neutron diffraction data (GEM, Bank 3, mean scattering angle $2\theta = 34.96°$) of $SrRu_2O_6$ with the magnetic contribution offset below. Tick marks denote positions of nuclear ($P\bar{3}1m$, red) and magnetic ($P\bar{3}1c$, green) Bragg reflections. Inset: the antiferromagnetic ordering of Ru atoms.

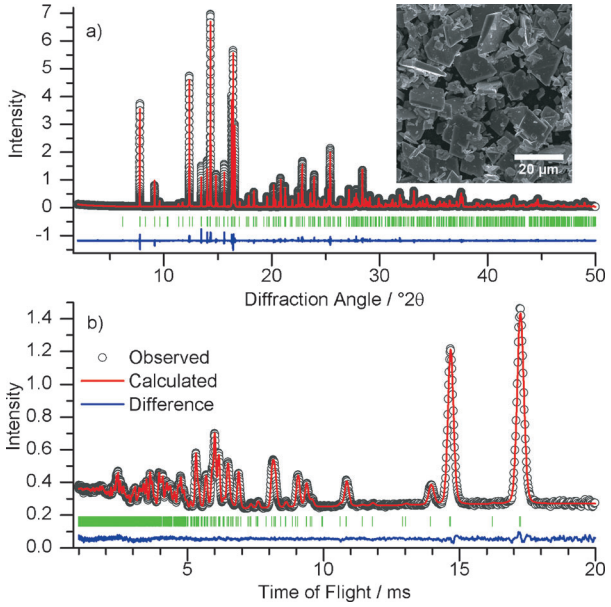

Figure 5. Rietveld refinements of $Ba_2Ru_3O_9(OH)$ using room temperature a) synchrotron XRD ($\lambda = 0.827154$ Å) and b) neutron diffraction data (GEM, Bank 3, mean scattering angle $2\theta = 34.96°$). Tick marks denote positions of expected reflections for space group $P2_12_12_1$, $a = 12.19451(1)$, $b = 9.87825(1)$, and $c = 7.05847(1)$ Å. Inset: a scanning electron micrograph of rhombohedral $Ba_2Ru_3O_9(OH)$ crystals.

solved initially by direct methods and refined against both powder XRD and powder neutron diffraction data (Figure 5b). It can be viewed as corrugated layers of edge- and corner-sharing RuO_6 octahedra with Ba^{2+} and H^+ ions projecting into the space between the layers. Its structure can be compared to $Ba_4Ru^{IV}{}_3O_{10}$,[32] an orthorhombic barium ruthenate that also consists of layers of RuO_6 quasi trimeric units interconnected in a corner-sharing manner. Whilst in $Ba_4Ru_3O_{10}$ these trimers are face-sharing and link to each other at one vertex to form a checkered structure, in $Ba_2Ru_3O_9(OH)$ the octahedra are part of edge-sharing trimers, and one octahedron from a trimer corner-shares with two octahedra in its neighboring trimer. Ru K-edge XANES spectroscopy confirms an average oxidation state of close to +5, Figure 2, while bond valence sums give Ru oxidation states of 4.85, 5.18, and 5.10 for each of the three crystallographic Ru sites. The thermal decomposition of $Ba_2Ru_3O_9(OH)$ to $BaRuO_3$ and RuO_2 occurs at around 500 °C, as seen by in situ powder XRD (Supporting Information, Figure S10).

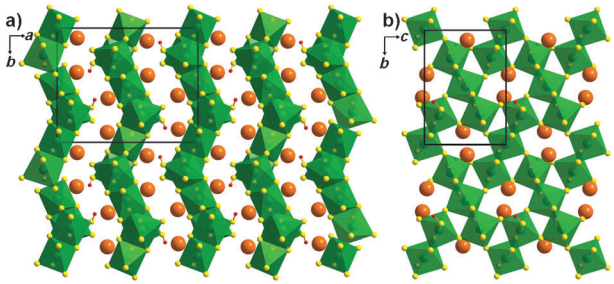

Figure 6. a) Structure of $Ba_2Ru_3O_9(OH)$ viewed along the *c*-direction, with Ba atoms in orange, green RuO_6 octahedra, and H atoms in red. b) One layer of RuO_6 octahedra viewed along the *a*-direction.

The magnetic properties of the new ruthenates were studied. The temperature dependence of the magnetic

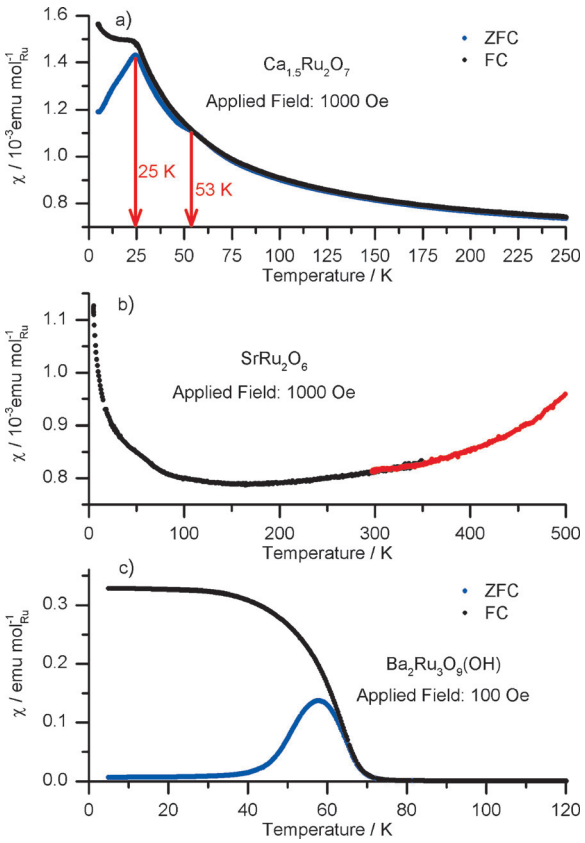

Figure 7. Magnetic susceptibility as a function of temperature of a) $Ca_{1.5}Ru_2O_7$, b) $SrRu_2O_6$, and c) $Ba_2Ru_3O_9(OH)$. In (a), features discussed in the text are indicated, and in (b) data were collected in two series of measurements: 500–300 K is shown in red and the low-temperature data (350–5 K) are shown in black.

susceptibility χ of $Ca_{1.5}Ru_2O_7$ (Figure 7a) is indicative of magnetic frustration at 25 K, similar to that previously reported for $Ca_2Ru_2O_7$.[16] An additional anomaly at about 53 K corresponds to the onset of hysteresis, indicative of possible spin glass-like behavior; this is supported by heat capacity measurements that show no phase transitions over these temperatures (Supporting Information, Figure S14). At temperatures above this transition the field-cooled (FC) susceptibility can be modeled using the Curie–Weiss law with an added temperature independent term, χ_0 and a Weiss temperature, θ, of −13(2) K, indicative of antiferromagnetic correlations. The observed moment μ per Ru is 0.36 μ_B, which is identical to the reported Ru moment for $Ca_2Ru_2O_7$,[16] but an order of magnitude smaller than the spin-only value for d^3 or d^2 metal ions, 3.87 and 2.83 μ_B, respectively. $SrRu_2O_6$ shows no clear transition temperature up to 500 K (Figure 7b; the sample decomposition makes susceptibility measurements at higher temperatures problematic), indicating that antiferromagnetic order persists well above room temperature. Furthermore, the susceptibility does not appear to exhibit a paramagnetic temperature dependence and there is a slight upturn at elevated temperatures, further indicating that it is antiferromagnetically ordered. The small upturn in susceptibility upon cooling to low temperature, beginning at 70 K, may be assigned to uncompensated spins, or due to impurity rutile RuO_2, although none is detected by diffraction. Figure 7c shows the temperature dependence of the magnetic susceptibility of $Ba_2Ru_3O_9(OH)$. Fitting to a modified Curie–Weiss function gives a Weiss temperature of 84(1) K, which is consistent with the Ru^V moments being ferromagnetically ordered. The observed Ru moment is 0.73 μ_B, which like the Ru moment in $Ca_{1.5}Ru_2O_7$ and $SrRu_2O_6$ is much smaller than expected for a d^3 metal ion in an octahedral environment.

In conclusion, three new ruthenium(V)-containing oxides with diverse structures have been prepared directly by mild temperature hydrothermal synthesis, with use of a combination of oxidizing reagents. A defective pyrochlore, $Ca_{1.5}Ru_2O_7$, with $Ru^{V/VI}$ occupying the B-site, shows glassy magnetic behavior. $SrRu_2O_6$ is a layered oxide that exhibits an unusually high antiferromagnetic ordering temperature. $Ba_2Ru_3O_9(OH)$, a layered material constructed from trimeric Ru^V octahedral units, is a ferromagnetic oxide. All of these oxides are metastable and decompose at temperatures far lower than typically used in conventional solid-state synthesis, demonstrating the effectiveness of low temperature solution-based methods in discovering new, kinetically stable compounds, in this case stabilizing high oxidation state ruthenates that have interesting magnetic properties. While these metastable oxides may not be suited to high temperature heterogeneous (solid–gas) catalysis applications, their use in electrocatalytic applications at ambient temperature would not be compromised. As can be seen in the SEM images presented, the materials are prepared as well-dispersed, faceted crystallites, and this may be of benefit for such applications. The synthesis method we disclose could easily be extended to the oxides of other precious metals, taking advantage of reactive, high-oxidation-state precursors, and the new barium ruthenate hydroxide could potentially be prepared as other precious-metal oxide analogues, such as Ir^V or Os^V, yielding novel magnetic materials. We are currently exploring these ideas.

Experimental Section

In a typical synthesis, $KRuO_4$ (1 mmol, Alfa Aesar, 98%) and the appropriate amount of MO_2 (M = Ca, Sr, Ba; Sigma; 75%, 98%, 95% respectively) were added to distilled water (10 mL). The mixtures were sealed in 23 mL Teflon-lined steel autoclaves and heated to 200 °C for 24 h in a preheated fan oven. The samples were then cooled and the resulting precipitates were recovered by suction filtration and washed with dilute HCl, distilled water, and acetone to facilitate drying. Synchrotron powder XRD data were collected using beamline I11,[33] at Diamond Light Source, U.K, using an X-ray wavelength of 0.827154 Å. Time-of-flight neutron powder diffraction experiments were carried out on the GEM instrument,[34] at ISIS, U.K. from powdered samples in a 6 mm diameter cylindrical can made of vanadium. Structural refinement from powder diffraction data was performed using the GSAS suite of software.[35] The initial structural model for $Ba_2Ru_3O_9(OH)$ was obtained using direct methods in the program FOX.[36] Fullprof[37] was used to fit the magnetic Bragg reflections of $SrRu_2O_6$. Ru K-edge X-ray absorption spectra were collected on beamline B18,[38] at Diamond Light Source, U.K. Samples were diluted with polyethylene powder and pressed into pellets approximately 1 mm thick. Data were collected in transmission mode and spectra were normalized using ATHENA.[39] DC

magnetization measurements were carried out using a Quantum Design MPMS.

Received: November 21, 2013
Revised: January 21, 2014
Published online: March 18, 2014

Keywords: hydrothermal synthesis · magnetic properties · neutron diffraction · ruthenium · X-ray absorption spectroscopy

[1] H. Over, *Chem. Rev.* **2012**, *112*, 3356.
[2] N. F. Atta, A. Galal, S. M. Ali, *Int. J. Electrochem. Sci.* **2012**, *7*, 725.
[3] J. M. Zen, R. Manoharan, J. B. Goodenough, *J. Appl. Electrochem.* **1992**, *22*, 140.
[4] A. T. Ashcroft, A. K. Cheetham, J. S. Foord, M. L. H. Green, C. P. Grey, A. J. Murrell, P. D. F. Vernon, *Nature* **1990**, *344*, 319.
[5] W. Witczak-Krempa, G. Chen, Y. B. Kim, L. Balents, *Annu. Rev. Condens. Matter Phys.* **2014**, *5*, 57.
[6] C. Dussarrat, J. Fompeyrine, J. Darriet, *Eur. J. Solid State Inorg. Chem.* **1995**, *32*, 3.
[7] F. Grasset, C. Dussarrat, J. Darriet, *J. Mater. Chem.* **1997**, *7*, 1911.
[8] D. Fischer, R. Hoppe, K. M. Mogare, M. Jansen, *Z. Naturforsch. B* **2005**, *60*, 1113.
[9] K. M. Mogare, W. Klein, E.-M. Peters, M. Jansen, *Solid State Sci.* **2006**, *8*, 500.
[10] C. Dussarrat, F. Grasset, R. Bontchev, J. Darriet, *J. Alloys Compd.* **1996**, *233*, 15.
[11] M. Jansen, I. V. Pentin, J. C. Schön, *Angew. Chem.* **2012**, *124*, 136; *Angew. Chem. Int. Ed.* **2012**, *51*, 132.
[12] S. J. Mugavero, M. D. Smith, W.-S. Yoon, H.-C. zur Loye, *Angew. Chem.* **2009**, *121*, 221; *Angew. Chem. Int. Ed.* **2009**, *48*, 215.
[13] K. Ishida, H. Mukuda, Y. Kitaoka, K. Asayama, Z. Q. Mao, Y. Mori, Y. Maeno, *Nature* **1998**, *396*, 658.
[14] R. J. Bouchard, J. L. Gillson, *Mater. Res. Bull.* **1972**, *7*, 873.
[15] J. M. Longo, P. M. Raccah, J. B. Goodenough, *J. Appl. Phys.* **1968**, *39*, 1327.
[16] T. Munenaka, H. Sato, *J. Phys. Soc. Jpn.* **2006**, *75*, 103801.
[17] J. A. Mydosh, *Spin glasses: An Experimental Introduction*, Taylor & Francis, London, **1993**.
[18] A. Rabenau, *Angew. Chem.* **1985**, *97*, 1017; *Angew. Chem. Int. Ed. Engl.* **1985**, *24*, 1026.
[19] K. Sardar, J. Fisher, D. Thompsett, M. R. Lees, G. J. Clarkson, J. Sloan, R. J. Kashtiban, R. I. Walton, *Chem. Sci.* **2011**, *2*, 1573.
[20] K. Sardar, S. C. Ball, J. D. B. Sharman, D. Thompsett, J. M. Fisher, R. A. P. Smith, P. K. Biswas, M. R. Lees, R. J. Kashtiban, J. Sloan, R. I. Walton, *Chem. Mater.* **2012**, *24*, 4192.
[21] K. E. Stitzer, W. R. Gemmill, M. D. Smith, H.-C. zur Loye, *J. Solid State Chem.* **2003**, *175*, 39.
[22] W. R. Gemmill, M. D. Smith, H.-C. zur Loye, *Inorg. Chem.* **2007**, *46*, 2132.
[23] M. A. Subramanian, G. Aravamudan, G. V. Subba Rao, *Prog. Solid State Chem.* **1983**, *15*, 55.
[24] A. Castro, I. Rasines, M. C. Sanchez-Martos, *J. Mater. Sci. Lett.* **1987**, *6*, 1001.
[25] N. E. Brese, M. O'Keeffe, *Acta Crystallogr. Sect. B* **1991**, *47*, 192.
[26] A. Collomb, M. Gondrand, M. S. Lehmann, J. J. Capponi, J. C. Joubert, *J. Solid State Chem.* **1976**, *16*, 41.
[27] D. Orosel, M. Jansen, *Z. Anorg. Allg. Chem.* **2006**, *632*, 1131.
[28] N. G. Parkinson, P. D. Hatton, J. A. K. Howard, C. Ritter, F. Z. Chien, M.-K. Wu, *J. Mater. Chem.* **2003**, *13*, 1468.
[29] E. E. Rodriguez, F. Poineau, A. Llobet, B. J. Kennedy, M. Avdeev, G. J. Thorogood, M. L. Carter, R. Seshadri, D. J. Singh, A. K. Cheetham, *Phys. Rev. Lett.* **2011**, *106*, 067201.
[30] J. Hubbard, W. Marshall, *Proc. Phys. Soc. London* **1965**, *86*, 561.
[31] J. Mravlje, M. Aichhorn, A. Georges, *Phys. Rev. Lett.* **2012**, *108*, 197202.
[32] A. H. Carim, P. Dera, L. W. Finger, B. Mysen, C. T. Prewitt, D. G. Schlom, *J. Solid State Chem.* **2000**, *149*, 137.
[33] S. P. Thompson, J. E. Parker, J. Potter, T. P. Hill, A. Birt, T. M. Cobb, F. Yuan, C. C. Tang, *Rev. Sci. Instrum.* **2009**, *80*, 075107.
[34] A. C. Hannon, *Nucl. Instrum. Methods Phys. Res. Sect. A* **2005**, *551*, 88.
[35] A. C. Larson, R. B. Van Dreele, *Los Alamos National Laboratory Report LAUR* **1994**, 86.
[36] V. Favre-Nicolin, R. Cerny, *J. Appl. Crystallogr.* **2002**, *35*, 734.
[37] J. Rodríguez-Carvajal, *Physica B* **1993**, *192*, 55.
[38] A. J. Dent, G. Cibin, S. Ramos, A. D. Smith, S. M. Scott, L. Varandas, M. R. Pearson, N. A. Krumpa, C. P. Jones, P. E. Robbins, *J. Phys. Conf. Ser.* **2009**, *190*, 012039.
[39] B. Ravel, M. Newville, *J. Synchrotron Radiat.* **2005**, *12*, 537.

